Journal of Computer Assisted Tomography
7(6):954–959, December

Nuclear Magnetic Resonance (NMR) Imaging of Intracerebral Hemorrhage in the Acute and Resolving Phases

Jorma T. Sipponen, Raimo E. Sepponen, and Arto Sivula

Abstract: Nuclear magnetic resonance imaging of intracerebral hemorrhage revealed a considerable difference in the appearance of the bleedings in the acute and resolving phases. Attention is drawn to the shortening of the relaxation time T_1 within the first 2 weeks after the acute onset of symptoms with the location of the change at the periphery of the lesion. The change was most evident with T_1 dependent inversion recovery sequence ($IR_{1,500/400}$). With this pulse scheme the acute hemorrhage was visualized as a dark area during its early days. A bright zone, reflecting the shorter T_1, was not seen until the resolving phase at the end of the 1st week. Although its pathophysiological aspects are so far unknown, this finding may offer an opportunity for dating intracerebral hemorrhages. **Index Terms:** Brain, hemorrhage—Nuclear magnetic resonance—Computed tomography.

Nuclear magnetic resonance (NMR) imaging has been shown to be useful for the diagnosis of cerebrovascular events (1–3). Chronic subdural hematomas are clearly detected, even in the isodense phase, due to their particular NMR properties—short relaxation time T_1 and long relaxation time T_2 (3).

In earlier publications a short T_1 has been reported also in acute intracerebral hemorrhage (4). In order to investigate the development of the NMR findings in intracerebral hemorrhages, patients were examined in the first days following the event and, if possible, again some days later in the resolving phase. The results revealed a change in the NMR properties of the lesion during resolution.

MATERIALS AND METHODS

The prototype proton NMR imager (Instrumentarium Corporation, Helsinki, Finland) may be briefly characterized as follows. The strength of the main magnetic field is 0.17 T (7.13 MHz). Two-dimensional Fourier transformation (2DFT) is used as the imaging method. The slice thickness is approximately 10 mm and the original matrix consists of 128 × 128 image pixels. The imaging time varies from 3½ to 9 min depending on the pulse sequence used and on the averaging times.

The pulse sequences used in this study are summarized in Tables 1 and 2. The two pulse sequences, i.e., saturation recovery (SR) and inversion recovery (IR), are strongly dependent on T_1. The total cycle time in these sequences was 1,500 ms; the repetition time (TR_1) in the SR sequence and the time of inversion (TI) in the IR sequence were 400 ms. The SR sequence was used in the first nine patients and the IR sequence in the rest of the patients.

To obtain images which better reflect the proton concentration, the proton density (PD) sequence was employed. In this pulse sequence, pulses of 90° are repeated with a long TR. The long interpulse time reduces the T_1 dependence of this sequence in most biological tissues. In the pulse sequences (SR, IR, and PD) the data were collected by spin-echo 30 ms after the read pulses (TE = time to echo).

To obtain images with stronger T_2 dependence, a spin-echo sequence (SE) with a longer TE (= 100 ms) was used. With a long TR, tissues with high proton concentration and a long T_2 give the strongest signal intensity. Shortening of the TR to 500 ms also gives T_1 dependence with the same

From the NMR Laboratory (J. T. Sipponen and R. E. Sepponen) and the Second Department of Surgery (A. Sivula), Helsinki University Central Hospital, Helsinki, Finland. Address correspondence and reprint requests to Dr. Sipponen at NMR Laboratory, Pkl Rtg, Meilahti Hospital, Haartmaninkatu 4, 00290 Helsinki 29, Finland.

TABLE 1. *Pulse schemes used*

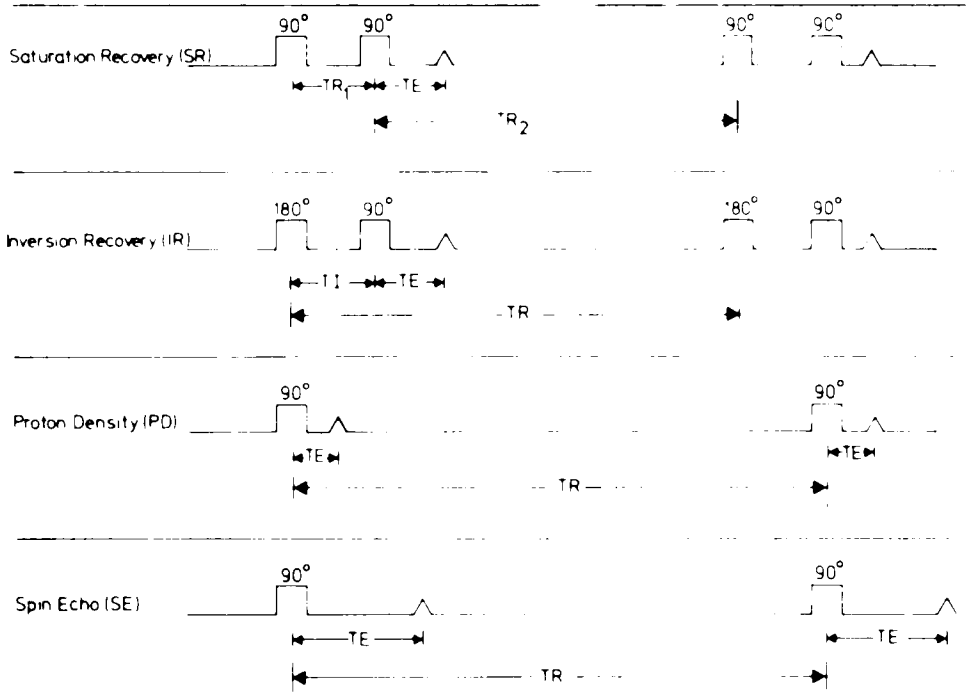

TR, TR_1, and TR_2 indicate time of repetition of the cycles. TI is time of inversion and TE is time to echo.

pulse sequence. Thus, tissues with high proton concentration and a long T_2 but a short T_1 give the highest intensity.

The signal intensity obtained is always a function of the different terms. The information from the tissues is conveyed by the interaction of the tissue NMR properties and the pulse sequence used. For the sake of clarity, the first-order approximations are given in Eqs. 1 to 3, where I, signal intensity; T_1, longitudinal (spin-lattice) relaxation time; T_2, transverse (spin-spin) relaxation time; TR_1, first time of repetition of the 90° pulses in the SR sequence; TI, time of inversion; TE, time to echo; and ζ, tissue proton concentration.

$$I_{SR} = \zeta \cdot e^{-TE/T_2}(1-e^{-TR_1/T_1}) \quad (1)$$

$$I_{IR} = \zeta \cdot e^{-TE/T_2}(1-2e^{-TI/T_1}) \quad (2)$$

$$I_{PD} \text{ and } _{SE} = \zeta \cdot e^{-TE/T_2}(1-e^{-TR/T_1}) \quad (3)$$

Thirteen patients (aged 29 to 75 years) with intracerebral hemorrhage were studied. A summary of the patients' data is presented in Table 3.

The CT examinations with either an EMI CT1010 head unit or a Siemens Somatom 2 were carried out in the acute stage in all patients. In one subject the CT study was repeated at 9 and in another at 13 days after the onset of symptoms. Nuclear magnetic resonance follow-up was possible in four patients as follows. One patient was scanned sequentially 2, 6, 13, and 28 days after the onset of the disease and in the other three patients reexamination was performed at 5, 9, and 10 days, respectively.

RESULTS

The clinical data and the most important findings, i.e., the visualization of the hemorrhage with the T_1

TABLE 2. *Time parameters used and the main contrast determinants*

	TR (ms)	TI (ms)	TE (ms)	Main contrast determinants
$SR_{1\ 500/400}$	400 (TR_1) 1,100 (TR_2)		30	T_1, proton density
$IR_{1\ 500/400}$	1,500	400	30	T_1, proton density
$PD_{2\ 000}$	2,000		30	Proton density
$SE_{2\ 000/100}$	2,000		100	T_2, proton density
$SE_{500/100}$	500		100	T_1, T_2, proton density

TABLE 3. *Summary of patients' data and visualization of lesion with T_1 dependent pulse sequences*

Patient/age (years) /sex	Etiology (if known) and location of the intracerebral hemorrhage	Time from the onset of symptoms to NMR imaging (days)	Visualization of the hemorrhage with $SR_{1,500/400}$ or $IR_{1,500/400}$
1/55/M	Right anterior cerebral artery aneurysm	28	Bright
2/48/M	Left anterior communicating artery aneurysm	1	Dark
3/29/M	Left frontal oligodendroglioma	9	Bright
4/52/F	Right temporal lobe	18	Bright zone with dark center
5/45/F	Right pericallosal artery aneurysm	1	Dark
6/62/F	Left temporoparietal lobe	1	Dark
7/75/M	Frontal lobes bilaterally	1	Dark
8/53/M	Left cerebellar hemorrhage	1	Dark
9/70/F	Right frontotemporal area	1	Mostly dark, small bright area
10/75/F	Right temporal lobe	1	Dark
		10	Bright
11/56/M	Right temporoparietal	2	Dark
		9	Bright
12/50/F	Right frontotemporal contusion	2	Dark
		5	Partially bright
13/52/F	Left temporal lobe	2	Dark
		6	Partially bright
		13	Bright
		28	Bright

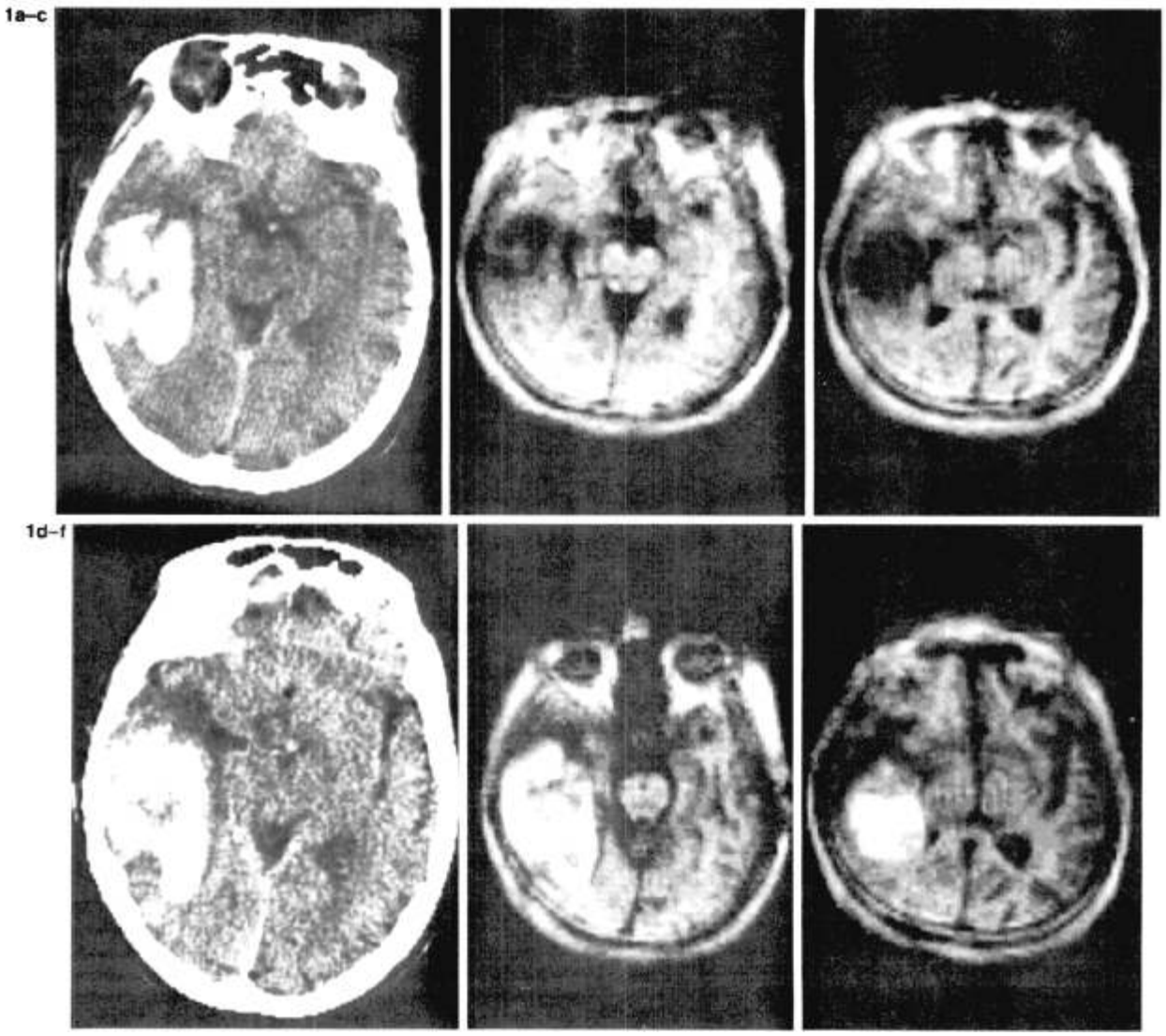

FIG. 1. *Patient 10.* Noncontrast CT **(a)** and two inversion recovery ($IR_{1,500/400}$) images **(b and c)** of a 75-year-old woman with an intracerebral hemorrhage 1 day after the onset of symptoms. Repeat CT **(d)** and IR **(e and f)** at 10 days indicate a considerable change in visualization of the hematoma in the resolving phase.

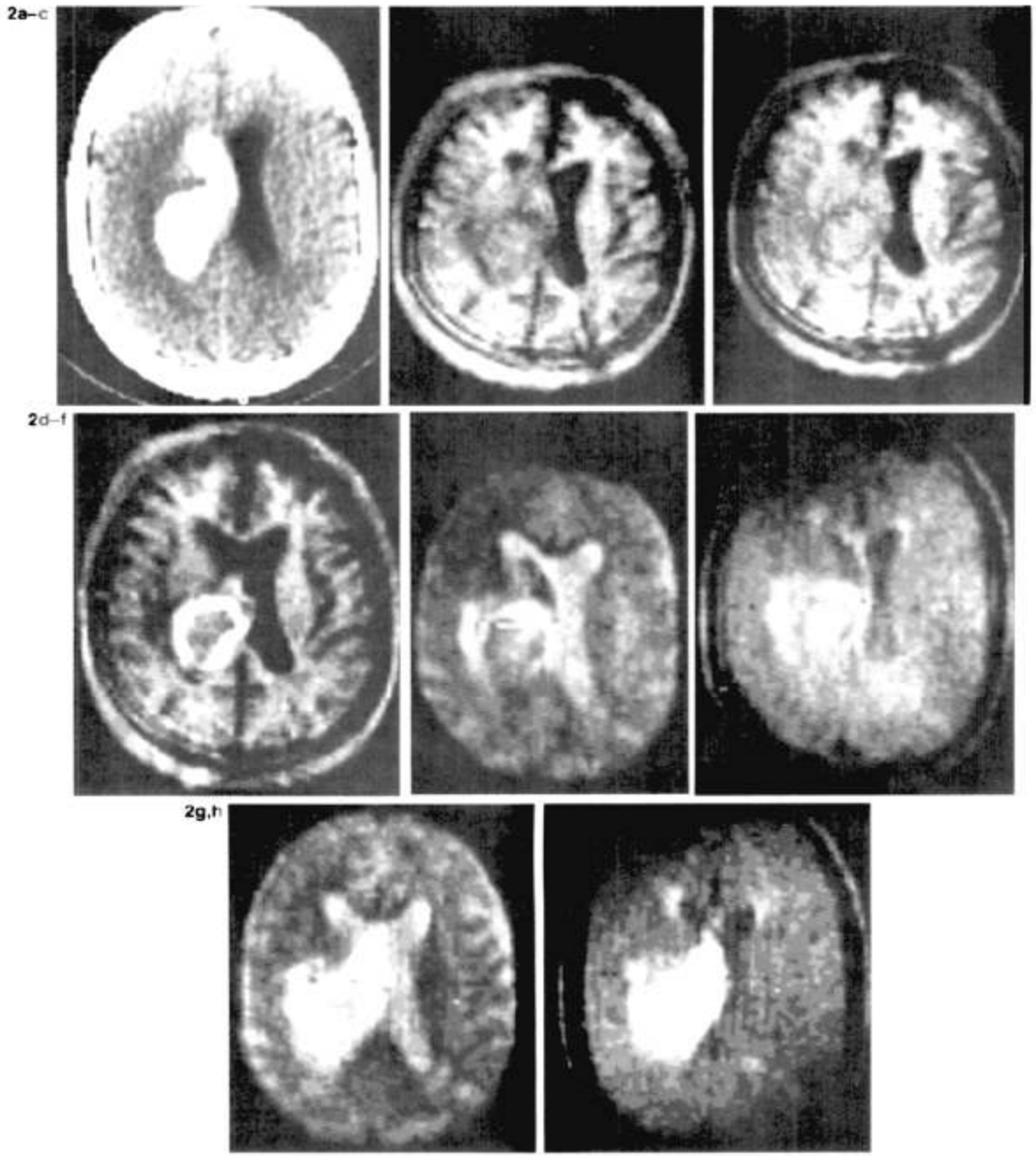

FIG. 2. *Patient 11.* Noncontrast CT **(a)** and inversion recovery ($IR_{1\,500\,400}$) **(b)** and $IR_{1\,500\,600}$ **(c)** images of a 45-year-old man with spontaneous intracerebral hemorrhage 2 days after the onset of symptoms. Repeat $IR_{1\,500\,400}$ image at 9 days **(d)**. Spin-echo ($SE_{2\,000\,100}$) and $SE_{500\,100}$ images at 2 days **(e and f)** and at 9 days **(g and h)**.

dependent pulse sequences $SR_{1,500\,400}$ or $IR_{1,500\,400}$, are summarized in Table 3. In nine patients in whom the examination was performed within 2 days from the onset of disease, the area of hemorrhage appeared dark. However, in examinations performed 5 days to 4 weeks after the onset of disease, bright areas could be demonstrated.

Three illustrative cases are presented in Figs. 1–3. The considerable change in the NMR appearance of the hemorrhage is clearly illustrated in Fig. 1. The intracerebral hemorrhage in this 75-year-old woman is shown by CT 1 day after the onset of symptoms (Fig. 1a). Two adjacent NMR sections with the $IR_{1,500\,400}$ sequence (Figs. 1b and c) show low intensity in the area of the hemorrhage. The patient was reexamined 9 days later with both CT and NMR. The NMR images at the same levels as the earlier examination revealed areas of very high intensity (Figs. 1d–f).

The NMR features of an intracerebral hemorrhage in a 56-year-old man are presented in Fig. 2, which includes the T_2 dependent spin-echo pulse

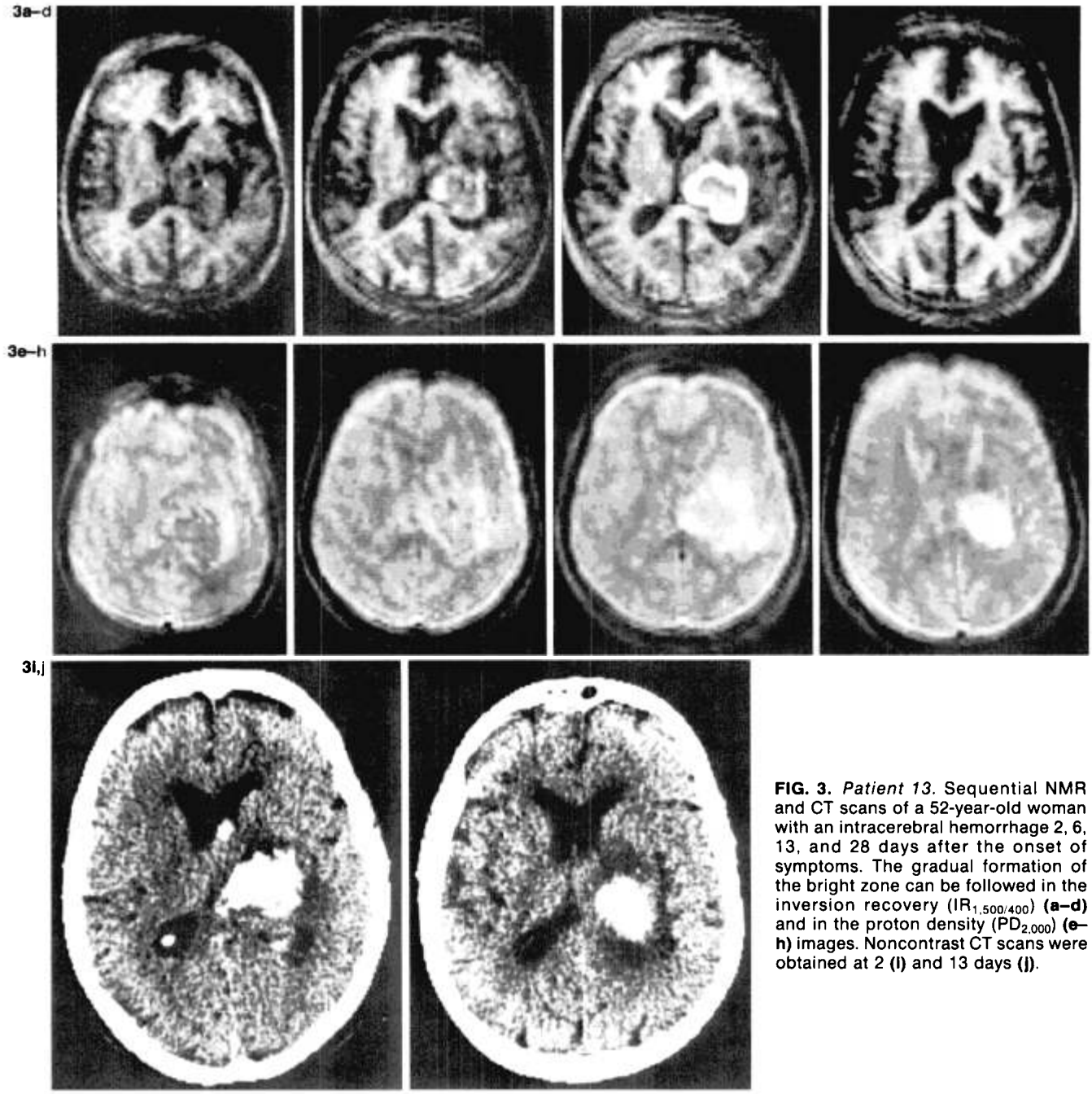

FIG. 3. *Patient 13.* Sequential NMR and CT scans of a 52-year-old woman with an intracerebral hemorrhage 2, 6, 13, and 28 days after the onset of symptoms. The gradual formation of the bright zone can be followed in the inversion recovery ($IR_{1,500/400}$) **(a–d)** and in the proton density ($PD_{2,000}$) **(e–h)** images. Noncontrast CT scans were obtained at 2 **(i)** and 13 days **(j)**.

sequence. The first examination was done 2 days after the acute onset of symptoms. Computed tomography demonstrated the intracerebral hemorrhage (Fig. 2a). The IR sequence was carried out with two time delays (TI) between the inversion and the read pulses. Using TI = 400 ms (Fig. 2b), a dark area with low intensity was found. On the other hand, with TI = 600 ms (Fig. 2c) the intensity of the lesion was about equal to that of the surrounding brain tissue. In the acute stage the $SE_{2,000/100}$ (Fig. 2e) demonstrates a bright intensity around the lesion. With this pulse sequence, tissues with a long T_2 and high proton concentration, such as the cerebrospinal fluid and tissue edema, show up as bright areas.

In Fig. 2f the same section is presented with the shortened cycle time ($SE_{500/100}$). Due to the rapid repetition rate, partial saturation of the long T_1 components ensues, and the cerebrospinal fluid appears dark. The tissues with a short T_1 are also seen in this sequence. The same patient was reexamined 1 week later. In the NMR images in this resolving phase the formation of a bright, bandlike zone with a short T_1 at the periphery of the lesion can be dem-

onstrated with the $IR_{1,500\,400}$ (Fig. 2d) and the $SE_{500\,100}$ (Fig. 2h) sequences. In the $SE_{2,000\,100}$ (Fig. 2g) the surrounding pure edema probably merges with the bright intensity zone of the lesion.

The gradual formation of the bright intensity zone with the $IR_{1,500\,400}$ sequence is well demonstrated in the patient who underwent sequential NMR scanning 2, 6, 13, and 28 days after the acute onset of symptoms (Figs. 3a–d). In these images the phenomenon can also be followed with the proton density images (Figs. 3e–h). The CT examination was performed in the acute stage (Fig. 3i) and was repeated 13 days after the onset of symptoms (Fig. 3j), when the resolving phase of the hematoma was underway.

DISCUSSION

The most unexpected finding was the rather long T_1 of the acute hemorrhage. The pulse sequence $IR_{1,500\,400}$ has been established as a standard scheme for differentiation between gray and white matter. Using this pulse sequence, most pathological processes are visualized as the dark areas due to their prolonged T_1. Chronic subdural hematomas, however, exhibit a short T_1 together with a long T_2; these hematomas are easily detected also in the isodense phase (3). Previous reports on NMR images in intracerebral hemorrhage have also stressed the short T_1 of the intracerebral hemorrhages (5–8). However, examinations carried out during the early days after the onset of the symptoms have probably not been included in these reports. This may explain the divergences from the findings in the present study.

Relaxation phenomena are dependent on the strength of the magnetic field. According to earlier spectroscopic studies, values of approximately 0.6 s can be expected for fresh blood at an applied radio frequency of approximately 7 MHz (9,10). Our findings appear to be consistent with these spectroscopic observations. In one of our patients a longer interpulse delay of 600 ms ($IR_{1,500\,600}$) (Fig. 2c) was used. This pulse sequence almost equalized the intensities of the lesion and that of the adjacent brain tissue. This finding also confirms the longer T_1 in the acute phase of the hemorrhage.

A considerable shortening of T_1 was observed in the four patients reexamined with NMR. The time sequence of this phenomenon can only be approximated on the basis of this study but the process seems to take some days (Figs. 3b–d). At the end of the 1st week the change was clearly detectable but partial. The intensity of the change increased up to the 2nd week and the ringlike zone was more complete. The dynamic nature of this process may give some hints about some pathophysiological aspects of this phenomenon.

Using the other pulse sequences, i.e., $PD_{2,000}$, $SE_{2,000\,100}$, and $SE_{500\,100}$, the changes and the typical location are also observed. Surrounding edema, visualized as hypodense areas on CT, has a long T_1 and exhibits dark intensity in the $IR_{1,500\,400}$ sequence. However, using an echo delay of 100 ms and a long TR ($SE_{2,000\,100}$), tissues with a high proton concentration and a long T_2 show up brightly. The differentiation with T_1 can also be achieved by shortening the cycle time to 500 ms ($SE_{500\,100}$). Using this pulse sequence, edema, due to its long T_1, is partly saturated and the intensities of the surrounding and inner parts of the hemorrhage are equalized (Fig. 2e). The brightest intensity in the outer part of the lesion is visualized later, in the resolving phase (Fig. 2h).

The cause of the above described NMR findings is unknown. The formation of a zone encircling the lesion at its periphery might hint at a process on the interface between the resolving hemorrhage and the adjacent brain tissue. The complex coagulation phenomena interplaying with biophysical aspects of NMR imaging may be responsible for the changing appearances of the evolving hematoma. The diagnostic implications of these findings are obvious.

Acknowledgment: This study was supported by the Academy of Finland and Instrumentarium Corporation, Helsinki, Finland.

REFERENCES

1. Sipponen JT, Kaste M, Sepponen RE, Kuurne T, Suoranta H, Sivula A. Nuclear magnetic resonance imaging in reversible cerebral ischemia. *Lancet* 1983;1:294–5.
2. Sipponen JT, Kaste M, Ketonen L, Sepponen RE, Katevuo K, Sivula A. Sequential nuclear magnetic resonance (NMR) imaging in patients with cerebral infarction. *J Comput Assist Tomogr* 1983;7:585–589.
3. Sipponen JT, Sepponen RE, Sivula A. Nuclear magnetic resonance (NMR) imaging in chronic subdural haematoma. Unpublished.
4. Bailes DR, Young IR, Thomas DJ, Straughan K, Bydder GM, Steiner RE. NMR imaging of the brain using spin-echo sequences. *Clin Radiol* 1982;33:395–414.
5. Doyle FH, Gore JC, Pennock JM, Bydder GM, Orr JS, Steiner RE, Young IR, Burl M, Clow H, Gilderdale DJ, Bailes DR, Walters PE. Imaging of the brain by nuclear magnetic resonance. *Lancet* 1981;2:53–7.
6. Bydder GM, Steiner RE, Young IR, Hall AS, Thomas DJ, Marshall J, Pallis CA, Legg NJ. Clinical NMR imaging of the brain: 140 cases. *AJR* 1982;139:215–36.
7. Crooks LE, Mills CM, Davis PL, Brant-Zawadzki M, Hoenninger J, Arakawa M, Watts J, Kaufman L. Visualization of cerebral and vascular abnormalities by NMR imaging: The effects of imaging parameters on contrast. *Radiology* 1982;144:843–52.
8. Young IR, Bailes DR, Burl M, Collins AG, Smith DT, McDonnell MJ, Orr JS, Banks LM, Bydder GM, Greenspan RH, Steiner RE. Initial clinical evaluation of a whole body nuclear magnetic resonance (NMR) tomograph. *J Comput Assist Tomogr* 1982;6:1–18.
9. Brooks RA, Battocletti JH, Sances A Jr, Larson SJ, Bowman RL, Kudravcev V. Nuclear magnetic relaxation in blood. *IEEE Trans Biomed Eng* 1975;22:12–8.
10. Pochobradsky J. Optimal field for detection of magnetically labelled blood. *J Magn Reson* 1982;48:163–75.